

Bending, free vibration and buckling of functionally graded carbon nanotube-reinforced sandwich plates, using the extended Refined Zigzag Theory

Original

Bending, free vibration and buckling of functionally graded carbon nanotube-reinforced sandwich plates, using the extended Refined Zigzag Theory / Di Sciuva, M., Sorrenti, M.. - In: COMPOSITE STRUCTURES. - ISSN 0263-8223. - STAMPA. - 227:(2019). [10.1016/j.compstruct.2019.111324]

Availability:

This version is available at: 11583/2749014 since: 2019-08-29T19:37:00Z

Publisher:

Elsevier

Published

DOI:10.1016/j.compstruct.2019.111324

Terms of use:

This article is made available under terms and conditions as specified in the corresponding bibliographic description in the repository

Publisher copyright

Elsevier postprint/Author's Accepted Manuscript

© 2019. This manuscript version is made available under the CC-BY-NC-ND 4.0 license
<http://creativecommons.org/licenses/by-nc-nd/4.0/>. The final authenticated version is available online at:
<http://dx.doi.org/10.1016/j.compstruct.2019.111324>

(Article begins on next page)

Applying q-Gaussians to the OH-stretching Raman bands of Water and Ice

Amelia Carolina Sparavigna¹✉

¹Department of Applied Science and Technology, Polytechnic University of Turin, Italy

In a previous discussion, we started showing how the q-Gaussian functions, also known as Tsallis functions, can be applied to the Raman spectroscopy investigations of the spectral region between 2800 and 3800 cm^{-1} , that is the OH-stretching Raman band of water. We decomposed the spectral region in three q-Gaussians. Being the q-parameter of q-Gaussians related to the correlation time of stochastic Kubo modelling of fluctuations, we proposed the use of this parameter to characterize the local environments of OH bonds. Here, we further discuss the OH-stretching Raman band of water and consider the same spectral region in the case of ice, to understand how the decomposition in q-Gaussians changes in the number of components and values of q-parameters.

Keywords: Raman Spectroscopy, q-Gaussian Tsallis Lines, Hydrogen Bonds, OH Stretching Band, Kubo Stochastic Model of Fluctuations

Introduction

In a previous work (Sparavigna, 2024), we have discussed some literature about the Raman spectroscopy of water, regarding the spectral region between 2800 and 3800 cm^{-1} , that is the region containing the OH stretching Raman band. We proposed the q-Gaussian functions, also known as Tsallis functions, to decompose the spectral region, identifying three q-Gaussian components. The q-Gaussian functions, also known as Tsallis functions, are depending on a parameter, the q-parameter, which is changing the shape of the function from Gaussian, for q close to 1, to Lorentzian for q=2. As shown in [ijsciences1](#), [ijsciences2](#), the q-Gaussian functions can be used to mimic the line shapes related to the stochastic Kubo modelling of fluctuations. Consequently, the value of the q-parameter can be linked to the time scale of dynamics (fast q=2, mid q=1.4 and slow q=1), related to the local environment of oscillating dipoles. Therefore, in our previous work, we started proposing the use of this q-parameter to characterize the local environments of water O-H bonds.

Here, we aim to further expand the use of q-Gaussians, by starting an investigation of the same spectral region in the case of ice, to understand how the decomposition in q-Gaussians changes in number of components and in values of q-parameters. We will show decompositions of the Raman spectra obtained by Đuričković et al., 2011, in their study of water-ice phase transition, and by Pershin and coworkers, 2015. However, before discussing ice, let us shortly summarize what we have previously considered in [Sparavigna, 2024](#). Moreover, we will add further discussions, especially regarding the

model of “interacting chromophores”, proposed by Auer and Skinner, 2008, a model which is based on Kubo stochastic approach.

Water OH stretching Raman bands

In our discussion about the spectral region between 2800 and 3800 cm^{-1} for water, we started from the work by Brewer et al., 2019, about the Raman spectroscopy of water and sea water. Water is made of simple molecules, which “are hydrogen bonded together forming molecular clusters. Rather little of the liquid water exists as the singlet H_2O molecule” (Brewer et al., 2019). As described by Brewer and coworkers, “water is in a state of temperature-controlled equilibrium between the hydrogen bonded (HB) and the nonhydrogen bonded (nHB) forms”. The nHB form is that of free H_2O molecule, and the different HB forms are “in a rapidly exchanging continuum of configurations” where the dominant form is the pentamer (H_2O)₅ (Brewer et al., 2019, Walrafen, 1964, Keutsch & Saykally, 2001, Smith et al., 2005).

After a brief review of literature, Brewer and coworkers reported their spectroscopic experiments, the spectra of which they decomposed in five Gaussian components. Walrafen, in 1964, identified three bands between 2800 and 3800 cm^{-1} , then he reported about four bands (Walrafen, 1967) and finally five Gaussian bands in 1986 (Walrafen et al., 1986). More recently, Carey and Korenowski (1998) and Furić et al., (2000) have used five Gaussian peaks too. About one of these bands, that centered at 3052 cm^{-1} , Brewer and coworkers report it as attributable to the $2\nu_2$ overtone of the bending vibration (Furić et al., 2000). Maeda and Kitano,



1995, tell this overtone being a “Fermi resonance with the first overtone of the bending motion of the H₂O molecule”. The “influence of Fermi resonance has recently been shown to be weak or absent, and today this idea seems obsolete” (Maeda and Kitano, mentioning Hare and Sorensen, 1992).

In Hu et al., 2013, we find told that the OH stretching vibration “is most informative about structure of water” (Hu et al., mentioning Maeda & Kitano, 1995), and this broad band “is usually deconvoluted into several components for analysis, commonly less than six”, as the five Gaussians by Carey and Korenowski. “Nevertheless, controversy on the quantity and assignment of components still remains” (Hu et al., 2013). For instance, Zhelyaskov et al., 1989, decomposed the OH stretching spectral region “into four isotropic components and three anisotropic components applying Fourier deconvolution. Some other researchers decomposed the contour into four components” (Hu et al., 2013, mentioning Li et al., 2003). Li et al., 2004, fitted the band with five Gaussian components, which have been assigned to molecules with are fully or partly hydrogen bonded. Qiang Sun, 2009, 2010, “classified the local hydrogen bonding of water molecule as DDAA (double donor–double acceptor), DDA (double donor–single acceptor), DAA (single donor–double acceptor) and DA (single donor–single acceptor) and free OH, which correspond to five deconvoluted Gaussian sub-bands of O–H stretching vibrational band of water” (Hu et al., 2013). Đuričković et al., 2011, “held that it was unnecessary to fit the spectrum and they directly analyzed the raw spectra without any deconvolution. In practice, the method applied in treating the spectra can be an art depending on the hypothesis on the identification of possible species or conformations in water” (Hu et al., 2013). Also Georgiev and coworkers stressed the decomposition method as being limited; the limit is the “necessity of making a preliminary assumption concerning the number and the shape of the component” (Maeda and Kitano, mentioning Georgiev et al., 1983).

In Maeda and Kitano, 1995, we can find also told that “Scherer et al. interpreted the OH stretching band of water in terms of four Gaussian components, which were attributed to symmetric and antisymmetric OH stretching vibrations of a symmetrically hydrogen-bonded and an asymmetrically hydrogen-bonded complex. In Maeda and Kitano, we can find described all the bands of the water Raman spectrum. “Raman scattering from liquid H₂O consists of the OH stretching vibration band (2800-3400 cm⁻¹), the ν_2 bending band near 1645 cm⁻¹, the combination of bending and libration bands ($\nu_2+\nu_L$) near 2100 cm⁻¹, and intermolecular fluctuation bands in the low-frequency regions which are due to the interaction between water molecules

through the hydrogen bonds” (Maeda & Kitano, 1995). For what is regarding the low frequency region, Faurskov Nielsen, 2001, is mentioning that Raman spectroscopy is a fast technique, so that the Raman picture can be related to a “fixed water structure”, that is, “a hydrogen-bonded network with a continuous breaking and making of hydrogen bonds”.

Gaussian–Lorentzian curves

About decomposition of the OH stretching band of water, let us consider also the article by Baumgartner and Bakker, 2009. The study proposed by Baumgartner and Bakker considers a method for analyzing the Raman spectra of synthetic pure water and saline fluid inclusions based on Gaussian–Lorentzian functions. The decomposed spectra are used “to determine the salinity of natural aqueous fluids”. The considered spectral region is the OH-stretching one. “This region shows a broad undulating elevated signal, which is a complex profile of overlapping bands. These bands can be defined according to a variety of theoretical vibrational modes such as unperturbed-, symmetric-, antisymmetric-, bending-vibrations and overtones. Multiple Gaussian–Lorentzian functions can be used to deconvolve [decompose] this composite spectrum. However, many possibilities for fitting this stretching region are published in the literature”, and Baumgartner and Bakker mention the five Gaussian components by Carey and Korenowski (1998), Furić et al. (2000), Li et al. (2004), Chumaevskii et al. (2001), the four components by Rull (2002) and the three components by Gopalakrishnan et al. (2005). “Therefore, the spectral analyses of the “stretching” region are far from straightforward” (Baumgartner & Bakker, 2009).

Gopalakrishnan et al. and coworkers use the following spectral assignments. “The broad peaks in the 3000-3600 cm⁻¹ region contain two prominent bands in the SFG [Sum Frequency Generation], Raman, and IR spectra of neat water and are positioned at ~3250 and ~3450 cm⁻¹. Generally following spectral assignments for ice [Buch & Devlin, 1999], and considering the increase in disorder of a noncrystalline system, the 3250 cm⁻¹ peak in the Raman (3253 cm⁻¹) and IR (3215 cm⁻¹) spectra is attributed to the vibrational modes from four oscillating dipoles of four-coordinate hydrogen-bonded water molecules. These collective vibrations can be viewed as possessing symmetric character. ... [Gopalakrishnan et al. and coworkers] assign the 3450 cm⁻¹ peak in the Raman, IR, and SFG spectra to the more asymmetrically oscillating dipoles from four-coordinate hydrogen-bonded water molecules. This spectral region can also be described as arising from four coordinate water molecules where one hydrogen is a poor hydrogen bond donor” (Gopalakrishnan et al., 2005). Gopalakrishnan et al. and coworkers use three

Gaussians fitted Raman spectra: two Gaussians are related to the two assignments given above, the third (smallest) component is given according to Scherer et al., 1973.

Baumgartner and Bakker, 2009, conclude that “The Raman spectrum of aqueous solutions (H₂O-NaCl mixtures) can be analysed by deconvolution into three Gaussian–Lorentzian contributions. Pure H₂O has peak positions at 3,223cm⁻¹ (Peak1), 3,433cm⁻¹ (Peak2), and 3,617cm⁻¹ (Peak3). The presence of salt in the aqueous solutions has significant influence on the morphology of the spectra”. To describe the spectral components, Baumgartner and Bakker used a linear combination of Gaussian and Lorentzian profiles:

$$I = \varphi I_{Gauss} + (1 - \varphi) I_{Lorentz}$$

This equation represents an “intensity fractionation” (φ). When $\varphi = 1$ we have a purely Gaussian contribution, and when $\varphi = 0$ a purely Lorentzian component. The lineshape coming from a linear combination of Gaussian and Lorentzians profile is known as pseudo-Voigt lineshape too. This profile is characterized by Lorentzian wings. Let us note that q-Gaussians have wing behaviors characterized by the q-parameters, with different power-law profiles according to the q values.

Three cases of water q-Gaussians decomposition

Since the research is open to different approaches, in Sparavigna, 2024, we proposed to use the q-Gaussian functions also for the analysis of water Raman spectra. For Raman spectra previously considered (Sparavigna, 2023, 2024), the fitted q-Gaussian functions were successfully in several cases, for instance graphite, ChemRxiv1, SERS spectra, ChemRxiv2, and so on, SSRN. The q-Gaussians, also known as “Tsallis functions”, are probability distributions derived from the Tsallis statistics (Tsallis, 1988, 1995, Hanel et al., 2009). The q-Gaussians are based on a generalized form of the exponential function (see discussion in Sparavigna, 2022), characterized by a continuous parameter q in the range $1 < q < 3$. As given by Umarov et al., 2008, the q-Gaussian is based on function $f(x) = Ce_q(-\beta x^2)$, where $e_q(\cdot)$ is the q-exponential function and C a constant. The q-exponential has expression:

$$\exp_q(u) = [1 + (1 - q)u]^{1/(1-q)}$$

The function $f(x)$ possesses a bell-shaped profile. In the case that we have the peak at position x_0 , the q-Gaussian is:

$$\text{q-Gaussian} = C \exp_q(-\beta(x - x_0)^2) =$$

$$C[1 - (1 - q)\beta(x - x_0)^2]^{1/(1-q)}$$

For q equal to 2, the q-Gaussian is the Cauchy-Lorentzian distribution (Naudts, 2009). The lineshape

is that corresponding to a homogeneous broadening of the lineshape. For q close to 1, the q-Gaussian is a Gaussian. The related lineshape corresponds to an inhomogeneous line broadening. For the q-parameter between 1 and 2, the shape of the q-Gaussian function is intermediate between the Gaussian and the Lorentzian profiles.

Let us show three cases from Sparavigna, 2024. One is regarding data by Baschenko and Marchenko, 2011. These researchers say that the water spectra can be approximated by four (or five) Gaussian-shaped peaks with positions at 3070, 3230, 3440, 3600 (and 3650) cm⁻¹. The Figure 1 in Sparavigna, 2024, shows that the OH stretching region given by Baschenko and Marchenko, 2011, can be decomposed using three q-Gaussians.

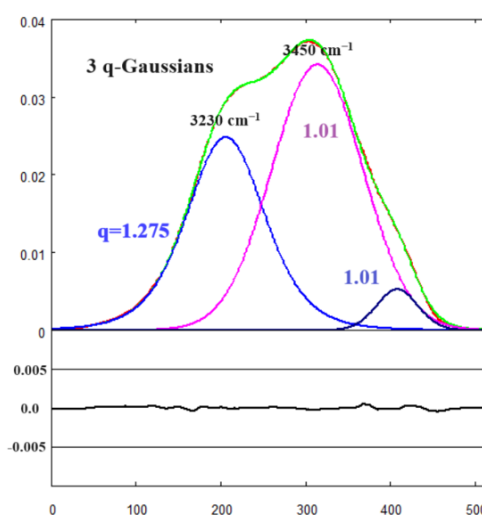


Fig.1: The Raman spectrum, shown in the Figs. 2 and 3 of Baschenko and Marchenko, is here proposed with a red line. It is decomposed by means of three q-Gaussians (magenta and blue colors). The green line is representing the sum of these q-Gaussians. Their q-parameters are given in the figure. Value $q=1.01$ is giving a q-Gaussian function which is numerically indistinguishable from a Gaussian. In the lower part of the figure, the difference between data and the sum of q-Gaussian functions is given. The center of the blue component ($q=1.275$) is about 3230 cm⁻¹, the center of the magenta component ($q=1.01$) is about 3450 cm⁻¹. Note please that data and q-Gaussians are given as functions of integers n (equally spaced points used in retrieving and fitting data), for the x-axis which is representing the Raman shift. A convenient scale is used for the y-axis (intensity axis).

In Fig.1, the magenta q-Gaussian curve is in good agreement with the decomposition proposed by Baschenko and Marchenko (also in their Figs. 2 and 3 this is the main component). In the Figure 1, our “data” are the intensity values that we can retrieve from the Figure 2 of Baschenko and Marchenko, interpolated to have the red line shown in the plot. Data and q-Gaussians are given as functions of integers n, equally spaced points used in retrieving and fitting data from the figures by Baschenko and Marchenko, for the x-axis which is representing the Raman shift. A convenient scale is used for the y-axis (intensity axis). The same we will do for all the

figures here proposed. The fitting calculation is obtained by minimizing the sum of the squares of the deviations Σ (sum from $n=1$ to $n=520$ in Fig.1) of the green points from the red data. In the case of Fig.1, $\Sigma = 1.44 \times 10^{-5}$.

The second case of decomposition in q-Gaussians that we are here showing is that regarding the Raman spectrum of bulk water we can find in a recent article by Malfait et al., 2022, Figure 2. This article is proposing the Raman spectra of water confined in mesoporous silica. Using the spectral band of bulk water given by Malfait et al., we obtain the fit shown in our Figure 2, where a decomposition in three q-Gaussians is given.

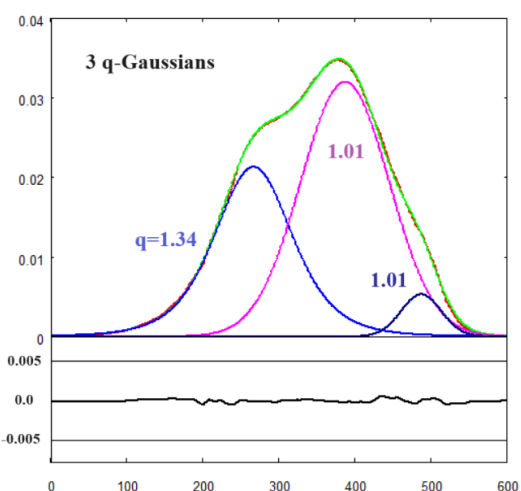


Fig.2: The Raman spectrum in the OH stretching region from the data given in the Figure 2 by Malfait et al., 2022, for bulk water. The data recovered from the figure are here proposed with red points, decomposed by three q-Gaussians (magenta and blue colors). The green line is representing the sum of these q-Gaussians. In the lower part of the figure, the misfit is proposed. Note please that data and q-Gaussians are given as functions of integers n (equally spaced points used in retrieving and fitting data), for the x-axis which is representing the Raman shift. A convenient scale is used for the y-axis (intensity axis).

Malfait and coworkers describe the OH stretching Raman band in the following manner. “Spectra of bulk water and confined water exhibit qualitatively the same shape, composed of a broad triple hump extending over this selected spectral region” (Malfait et al., 2022). In their Figure 3, the researchers are proposing the use of three Gaussians to evidence a first component “generally associated with the O–H stretching vibration of water molecules involved in a tetrahedral structure” (that is the blue component $q=1.34$ in our Fig.2), and a second component which “corresponds to the distorted H-bond network” (Malfait and coworkers mentioning D’Arrigo et al., 1981). This second component is our magenta $q=1.01$ q-Gaussian in Fig.2. The third component “is related to the O–H stretching of water molecules that are not involved in intermolecular HB (named free water)” (Malfait et al., 2022). This is the blue shoulder in the Fig.2 on the right.

In the following Figure 3, the third q-Gaussian decomposition is made for the plot by <https://www.stellarnet.us/application-note-raman-spectrum-water/>.

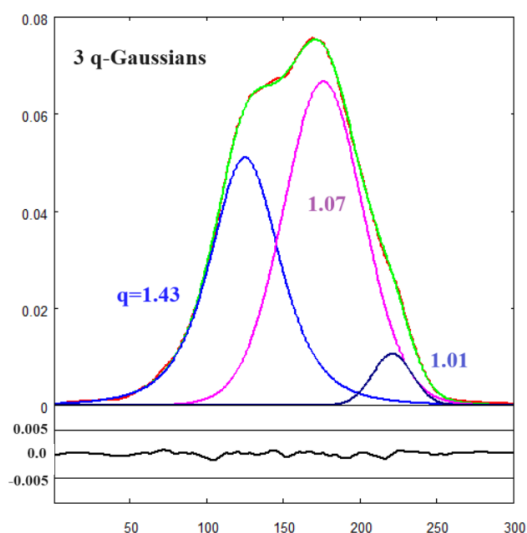


Fig.3: The Raman spectrum from [stellarnet.us](https://www.stellarnet.us) is here proposed with red points, decomposed by three q-Gaussians (magenta and blue colors). The green line is representing the sum of these q-Gaussians.

The web site (archived) is talking about the Raman scattering spectrum of pure water in the following manner. “The shoulder at $\sim 3250 \text{ cm}^{-1}$ [here in the Fig.2, the blue component on the left] corresponds to the asymmetric OH stretch, and the most intense feature at $\sim 3410 \text{ cm}^{-1}$ [magenta] corresponds to the symmetric OH stretch. Even more intriguing, there is a small shoulder at $\sim 3630 \text{ cm}^{-1}$ [the blue component on the right] which corresponds to the OH stretch of a water molecule which is only partially involved in hydrogen bonding – a particularly rare event.” In the figure, the web site is representing two molecules in symmetric and asymmetric (in fact, antisymmetric) mode vibrations.

Symmetric and antisymmetric modes

Having mentioned the symmetry of modes, let us remember that Maeda and Kitano are also referring the interpretation of the spectrum proposed by Scherer et al., which is based on symmetric and antisymmetric OH stretching vibrations. Scherer and coworkers, 1974, introduced a “Two Species Model”. They “classify hydrogen-bonded water molecules into two categories”. They place “all those molecules that have strong hydrogen bonding on both their hydrogens, ...HOH..., in one category. The two O-H bonds are assumed to have equal or very nearly equal strengths. In the second category we place all those molecules that have one strong hydrogen bond and one very weak hydrogen bond, ...HOH..... . We [Scherer and coworkers] call a molecule in the first category a “symmetric complex,” and, a molecule in the second category an “asymmetric complex.” We

assume that there is a distribution of hydrogen-bond strengths for the strongly hydrogen-bonded OH... groups of both the symmetric and asymmetric complex. A second narrower distribution is assumed for the very weak hydrogen-bonded OH.... of the asymmetric complex. We expect that bonding of the lone pair electrons in H-O-H affects the strength of the O-H bond and that this contributes to the frequency shift and broadening of the associated OH stretching bands” (Scherer et al., 1974).

The Scherer and coworkers’ model can be easily compared with the model proposed by Carey, 1996. The OH stretching vibrational region is decomposed by Carey into four bands, the lowest of them, at $\sim 3240 \text{ cm}^{-1}$, “corresponds to a fully symmetric 4-hydrogen bonded tetrahedral water molecule where all neighboring water molecules are vibrating together in phase. When the “attached molecules are vibrating out of phase with each other”, we find a component at an energy of $\sim 3385 \text{ cm}^{-1}$. Then, due to the loss of one hydrogen bond, the OH stretching vibrations at an energy of approximately $\sim 3490 \text{ cm}^{-1}$ and $\sim 3620 \text{ cm}^{-1}$ appear (Carey, 1996). About the model, Carey is mentioning Monosmith and Walrafen, 1984.

Returning to the work by Scherer et al., 1974, the observed bands are attributed by Scherer and coworkers to the symmetric and antisymmetric OH stretching vibrations of symmetrically and asymmetrically hydrogen-bonded complexes (Scherer et al., 1974). The researchers analyzed the isotropic and anisotropic spectra obtained by means of polarized Raman spectroscopy. They “collected Raman scattering 90° (X) to the incident beam (polarized (Z)). The horizontal (Z) and vertical (Y) components were measured with a polaroid analyzer. The spectra were intensity corrected and transformed into isotropic and anisotropic spectra” (Scherer et al., 1974). The isotropic spectrum is told related to the mean polarizability derivative and the anisotropic spectrum to the mean anisotropy derivative. Indicating the isotropic and anisotropic spectra as I_α and I_β respectively, these spectra are defined as (see also Porezag and Pederson, 1996, and Smith and Dent, 2019):

$$I_{\text{obsd}}(\text{Y}(\text{ZZ})\text{X}) = I_\alpha + I_\beta$$

$$I_{\text{obsd}}(\text{Y}(\text{ZY})\text{X}) = 3 I_\beta / 4$$

The notation used is the “Porto notation”. This notation has the form A(BC)D, where A is the laser light propagation direction, B is the laser light polarization direction, C is the scattered Raman light polarization direction, D is the scattered Raman light propagation direction. In samples such as liquids and microcrystalline powders, the scattered light is made by a combination of light with polarization parallel and perpendicular to that of the excitation laser light. With the polarized Raman spectroscopy, the spectra of each component can be obtained so that, for a

given band, the ratio of perpendicular against parallel intensity can provide the “depolarisation ratio” (ρ). This ratio is related to the symmetry of the vibrational mode (Smith and Dent, 2019). For a totally symmetric vibrational band, ρ is less than 0.75. If ρ is greater than or equal to 0.75, the band is a depolarised band.

In Tukhvatullin et al., 2011, we find proposed an analysis of the polarized Raman spectra, which “allows one to make a conclusion that in the diffuse OH-band it is possible to extract contributions of symmetric and anti-symmetric vibrations of water molecules. The same conclusion can be made on the base of results of quantum-chemical simulations”. The “differently polarized components of the spectra were allocated using the analyzer and depolarizing plate, which were installed at the entrance slit of the spectrometer” (Tukhvatullin et al., 2011).

In their article, Tukhvatullin and coworkers conclude that the total band in the spectral region $3000\text{--}3800 \text{ cm}^{-1}$ of liquid water “is conditioned by the imposition of two bands corresponding to symmetric (weakly depolarized) and antisymmetric (depolarized component) vibrations. The terms “symmetric” and “antisymmetric” vibrations are valid for a single molecule of water. At the aggregation of molecules these terms lose their sense, but vibrations of this sort remain” (Tukhvatullin et al., 2011). Moreover, it is told that, for the gaseous water, these “two vibrational bands with frequencies of 3657 cm^{-1} and 3756 cm^{-1} are observed in IR absorption spectra. The first band belongs to the symmetric vibrations; the second band belongs to the antisymmetric ones”. In the Raman spectra, the depolarization ratios of the bands are different: “the high-frequency band (antisymmetric vibration) is the depolarized one; the low-frequency band (symmetric vibration) is the polarized one. The difference between the peak frequencies of the bands is about 100 cm^{-1} ”. Tukhvatullin and coworkers “note that this magnitude is significantly (almost twice) less than the difference in frequencies of components of the complex band in the spectrum of Raman scattering of liquid water”.

Vibrational chromophores

We have found literature stressing the role of symmetric and antisymmetric modes in determining the OH-stretch band. However, different conclusions have been proposed by Auer and Skinner, 2008. The researchers stress that, although “IR and Raman parallel- and perpendicular-polarized spectra in the OH stretch region for liquid water” are available for years, “their interpretation is still controversial”. Moreover, the “theoretical calculation of such spectra for a neat liquid presents a formidable challenge due to the coupling between vibrational chromophores and the effects of motional narrowing”. Auer and

Skinner proposed a molecular dynamics method based on ab initio models to approach “the calculation of couplings between chromophores”, to obtain the line shapes. According to Auer and Skinner, “results are in good agreement with experiment for the IR and Raman line shapes, and capture the significant differences among them”.

Auger and Skinner analysis “indicates that even though the coupling between OH stretch chromophores is relatively modest, the instantaneous vibrational eigenstates are delocalized over a substantial up to 12 number of chromophores. This delocalization has a profound impact on the spectroscopy, producing a collective mode centered at around 3250 cm^{-1} . The other characteristic frequencies appear as the peak in the local-mode distribution of frequencies at about 3490 cm^{-1} , and the shoulder in the same distribution at about 3650 cm^{-1} due to hydrogen atoms not involved in hydrogen bonds. ... Our [Auer and Skinner] analysis, which emphasizes the role of coupling between chromophores, indicates that for neat liquid H_2O spectral peaks cannot be meaningfully assigned to individual molecules in different molecular environments. Moreover, substantial symmetry breaking due to the local molecular environment means that the symmetric and antisymmetric normal modes of water are not a useful basis, and it is not meaningful to make spectral feature assignments based on these normal modes” (Auer and Skinner, 2008).

Therefore, we have to remark that isolated H_2O molecules have symmetric and antisymmetric vibrations, but “the vibrations of liquid H_2O are qualitatively different” (De Marco et al. 2016, mentioning Skinner et al.). In the liquid water, the “hydrogen-bonding interactions give rise to strong intermolecular coupling, which greatly influences the frequency of the O–H stretching and HOH bending modes and breaks the gas-phase symmetry. As a result, the high-frequency vibrational motions of H_2O are delocalized over multiple molecules, with exciton states (eigenstates) whose form depends explicitly on the extended structure of water’s fluctuating hydrogen-bond network” (De Marco et al. mentioning Jansen et al., 2005, Auer and Skinner, 2008, Torii, 2006, Choi and Cho, 2013, Paarmann et al., 2008).

Discussion

In Figures 1-4 in [Sparavigna, 2024](#), it had been shown that we have, for the lower frequency part of the OH stretching band, blue q-Gaussians with q values ranging from 1.018 to 1.43 (here in the Figures 1-3, we have $q=1.275$, 1.34 and 1.43). In [our previous discussion](#), we proposed that these q-Gaussians represent the “fully symmetric 4-hydrogen bonded tetrahedral water molecule where all

neighboring water molecules are vibrating together in phase” (Carey, 1996). With a q-Gaussian, we do not need to postulate the presence of a further component, as the Fermi resonance in Carey, 1996. The other main component, the magenta q-Gaussian, can correspond to “the loss of a hydrogen bond”, consequently accompanied by asymmetry. The last blue component on the right of the magenta component is due to the free OH stretching as in the vapor state. Therefore, a value of q-parameter greater than 1, is indicating the presence of a more regular environment, with respect to the Gaussian case. If we consider the model by Scherer et al., 1974, again we have the four components substituted by two q-Gaussians.

In the case of Auer and Skinner approach, 2008, we find interacting vibrational producing two main bands with a shoulder. The researchers started from the Kubo theory (1969), with its stochastic approach to the line shapes, to include interactions and determine the specific profiles of these bands. About Kubo theory for chromophores, in [Sparavigna, 2024](#), we considered Tokmakoff, 2014, who was focusing on “how the chromophore’s interactions with its environment influence its transition frequency and absorption lineshape”. Following Tokmakoff and other literature, in previous works ([ijsciences1](#), [ijsciences2](#)) we considered that the q-Gaussians can be used to represent the stochastic Kubo line shapes. Moreover, we can characterize the q-Gaussian functions in the framework of the time scale of fluctuations as follows. Since the q-Gaussians can be used to mimic the Kubo line shapes, the q-parameters can be linked to the local environments of the oscillating dipoles (vibrational chromophores). As a consequence, the value of the q-parameter turns out to be related to the time scale of dynamics (fast $q=2$, mid $q=1.4$ and slow $q=1$). Returning to the O-H stretching band, we could therefore consider that the blue q-Gaussian at about 3250 cm^{-1} is characterized by a modulation which is “faster” than that of the magenta component. It means that the local environments of the O-H bond, in the blue and magenta cases, are different. Further investigation is also interesting, in the framework of a q-Gaussian approach, for evidencing the existence of collective modes, such as in the case of the 3250 cm^{-1} band.

The water-ice transition

About the decomposition of the OH-stretching Raman band, Đuričković et al., 2011, asserted as unnecessary to fit it. Đuričković and coworkers directly analyzed the band without any deconvolution. In their work, the researchers used the Raman spectroscopy to study the liquid–solid water phase transition, with a special regard to the OH stretching band. Of the three spectral regions of water, that is translational/librational below 400 cm^{-1} , OH bending band around 1600 cm^{-1} , and OH

stretching band, Đuričković and coworkers decided to use the last band for two reasons: it is the most intense band and it is “closely related to the structure of water [Đuričković and coworkers, mentioning Bunkin et al., 2004, Kargovsky, 2006], and therefore its phase”.

To the OH-stretching modes of water contribute intramolecular and intermolecular O–H bonds. “Thus, the effects of both intramolecular and intermolecular vibrational couplings of the OH–sb [stretching band] are mingled. However, it is primarily the intermolecular coupling that characterizes the spectral response of water” (Đuričković et al., 2011, mentioning Auer and Skinner, 2008, and Sceats et al., 1979). “This bond being flexible, it is sensitive to temperature, [Đuričković et al., 2011, mentioning Becucci et al., 1999] explaining why the OH–sb was selected as relevant for the phase transition determination”.

Đuričković and coworkers tell the OH stretching band originated, in liquid water, “from the symmetric and asymmetric OH–stretching vibrations. The fact that this band is rather broad implies the need for its deconvolution into several components, and a large controversy about the number of components and their origins exists in the literature” (the researchers mentioned Wang et al., 2003, who studied spectral diffusion by ultrafast IR-Raman spectroscopy). As we have shown before, Sparavigna, 2024, - see also the three examples given above -, using q-Gaussians, three components are enough to decompose the band. The number of components is strictly related to the functions used for decomposition.

“The intramolecular O–H bonds are influenced by neighboring intermolecular hydrogen bonds, which are sensitive to the temperature and, therefore, to the phase”. Đuričković and coworkers note that vibrations are varying with the phase, so that the ice has a spectrum different from that of water in the liquid phase. “The temperature decrease induces a decrease in the intensity of the region above 3325 cm^{-1} corresponding to the asymmetric stretching and, by contrast, an increase of the intensity of the region below 3325 cm^{-1} corresponding to the symmetric OH– stretching”. With the phase transition, the spectrum changes its profile in the intensities and wavenumbers of the peaks. The decrease of temperature is producing a shift of the entire OH stretching band as shown by the Fig.2 by Đuričković and coworkers. The shift is caused by the change of specific volume at the phase transition. “This volume increase is likely caused by the elongation of the O–

H bonds in the ice, so that the wavenumber of vibrational modes diminishes” (Đuričković et al., mentioning Schmidt and Miki, 2007). Moreover, of the OH–sb, Đuričković and coworkers noted that the low wavenumber part, that they attribute to the symmetric stretching modes, is enhanced on cooling. “In liquid water, hydrogen bonds are constantly formed and broken due to their weakness compared to covalent ones”: when the temperature decreases, the thermal agitation reduces, such as the breaking of hydrogen bonds. “The structure then becomes more steady via the formation of new hydrogen bonds between the water molecules. Simultaneously, we observe a narrowing and an intensity increase of the spectral component centered at 3138 cm^{-1} , which becomes clearly defined in ice. This low wavenumber part of the OH–sb of water could be considered as the proper marker of the ice” (Đuričković et al., 2011).

Water and ice spectra by Đuričković et al. and by Pershin et al.

Let us consider the spectra of water and ice, proposed by Đuričković and coworkers in their Figure 5. Let us use the same approach to their data as in our previous Figures. The decomposition for water (it seems the spectrum being obtained at 10°C,) is given in the following Figure 4. We have three q-Gaussian components, one of which is quite smaller. In the Figure 5 we show the spectrum of ice at -10°C.

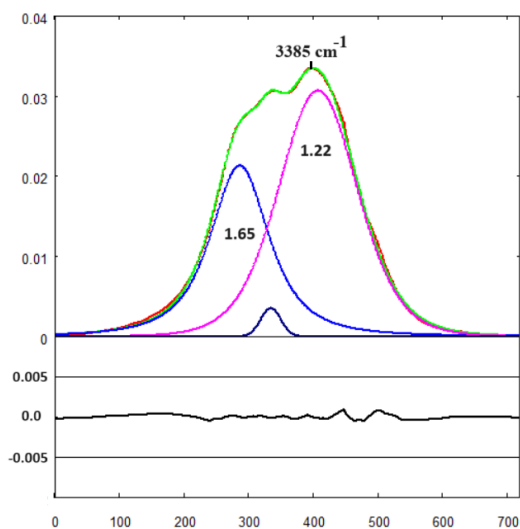


Fig.4: The Raman spectrum of liquid water in the OH stretching region from the data given in the Figure 5 by Đuričković et al., 2011. The data recovered from the figure are here proposed with red points, decomposed into three q-Gaussians (magenta and blue colors). The green line is representing the sum of these q-Gaussians. In the lower part of the figure, the misfit is proposed. The smallest component has $q=1.01$.

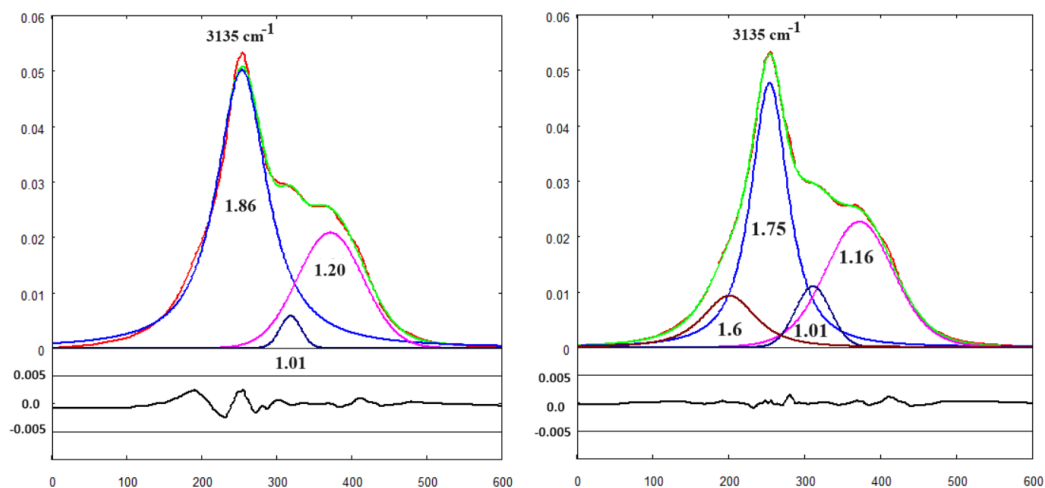


Fig.5: The Raman spectrum of ice in the OH stretching region from the data given in the Figure 5 by Đuričković et al., 2011. The data recovered from the figure are here proposed with red points, decomposed into three q-Gaussian (left, magenta and blue colors) and into four q-Gaussians (right, magenta, blue and dark red colors). The green line is representing the sum of these q-Gaussians. In the lower part of the figure, the misfit is proposed. Comparing left and right panels, it seems that a shoulder exists ($q=1.6$).

In the Figure 4, it is shown the fitted curve for water. The fitting calculation is obtained by minimizing the sum of the squares of the deviations Σ (sum from $n=1$ to $n=720$ in Fig.4) of the green points from the red data. In this case, $\Sigma = 4.9 \times 10^{-5}$. In the Figure 5 we consider the data regarding ice. The fitting calculation (right panel) gives Σ (sum from $n=1$ to $n=600$) as $\Sigma = 5.75 \times 10^{-5}$.

In Pershin et al., 2015, in their Fig.7, we can find “the detailed Raman OH-band profiles for ice and water in 7(a)”. “It is clearly observed that two phases can be easily distinguished using the OH-band profile”.

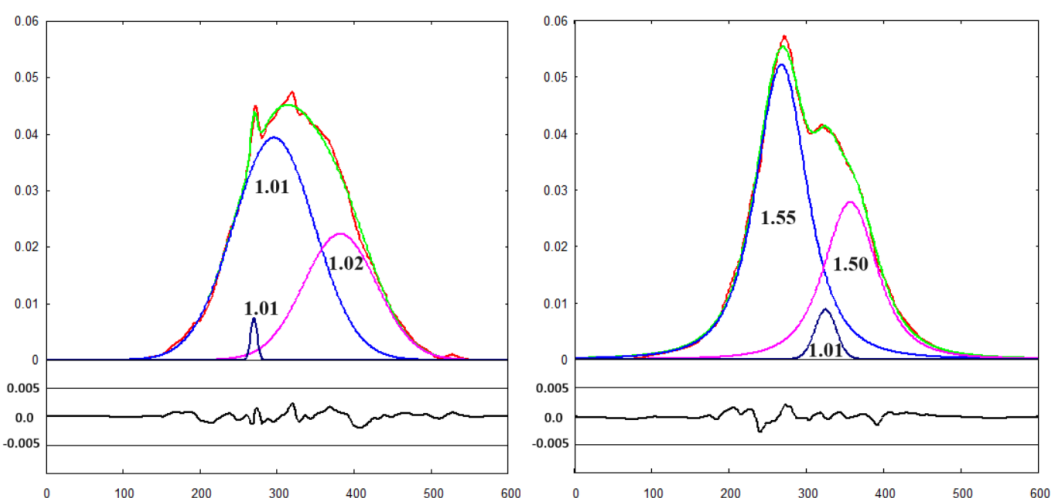


Fig.6: Left: Raman spectrum of liquid water in the OH stretching region from the data given in the Figure 7 by Pershin et al., 2015. The data recovered from the figure are here proposed with red points, decomposed into three q-Gaussians (magenta and blue colors). The green line is representing the sum of these q-Gaussians. In the lower part of the figure, the misfit is proposed. Right: Raman spectrum of ice in the OH-stretching region from the data given in the Figure 7 by Pershin et al., 2015. Note the increase of the values of the q-parameters.

Conclusion

As evidenced by the q-Gaussian decompositions given in the Figures 5 and 6 for the OH-stretching Raman band of ice, the solidification is accompanied by an increase of values of the q-parameters. As told in the case of liquid water, the q-parameter reflects the role of local environments on chromophores. The increase of local order is therefore inducing faster dynamics. In the case of the Figure 5, it seems that a left shoulder to the 3135 cm^{-1} peak exists. This

shoulder is negligible in the case of Figure 6. These two decompositions indicate that the use of q-Gaussians can be relevant for the Raman spectroscopy of ice too. Further studies are consequently required to increase the number of experimental cases.

References

1. Auer, B. M., & Skinner, J. L. (2008). IR and Raman spectra of liquid water: Theory and interpretation. *The Journal of Chemical Physics*, 128(22).

2. Baschenko, S. M., & Marchenko, L. S. (2011). On Raman spectra of water, its structure and dependence on temperature. *Semiconductor physics, quantum electronics & optoelectronics*, 14(1), 77-79.
3. Baumgartner, M., & Bakker, R. J. (2009). Raman spectroscopy of pure H₂O and NaCl-H₂O containing synthetic fluid inclusions in quartz—a study of polarization effects. *Mineralogy and Petrology*, 95(1), 1-15.
4. Becucci, M., Cavalieri, S., Eramo, R., Fini, L., & Materazzi, M. (1999). Accuracy of remote sensing of water temperature by Raman spectroscopy. *Applied optics*, 38(6), 928-931.
5. Benson, S. W., & Siebert, E. D. (1992). A simple two-structure model for liquid water. *Journal of the American Chemical Society*, 114(11), 4269-4276.
6. Brewer, P. G., Peltzer, E. T., & Walz, P. M. (2019). How much H₂O is there in the ocean? The structure of water in sea water. *Journal of Geophysical Research: Oceans*, 124(1), 212-226.
7. Buch, V., & Devlin, J. P. (1999). A new interpretation of the OH-stretch spectrum of ice. *The Journal of chemical physics*, 110(7), 3437-3443.
8. Bunkin, A. F., Pershin, S. M., & Rashkovich, L. N. (2004). Changes in the Raman spectrum of OH stretching vibrations of water in an ultrasonic cavitation field. *Optics and spectroscopy*, 96, 512-514.
9. Carey, D. M. (1996). Measurement of the Raman Spectrum of Liquid Water. United States. doi:10.2172/767069. <https://www.osti.gov/servlets/purl/767069>
10. Carey, D. M., & Korenowski, G. M. (1998). Measurement of the Raman spectrum of liquid water. *The Journal of Chemical Physics*, 108(7), 2669-2675. <https://doi.org/10.1063/1.475659>
11. Choi, J. H., & Cho, M. (2013). Computational IR spectroscopy of water: OH stretch frequencies, transition dipoles, and intermolecular vibrational coupling constants. *The Journal of Chemical Physics*, 138(17).
12. Chumaevskii, N. A., Rodnikova, M. N., & Sirotkin, D. A. (2001). Cationic effect in aqueous solutions of 1: 1 electrolytes by Raman spectral data. *Journal of Molecular Liquids*, 91(1-3), 81-90.
13. D'Arrigo, G., Maisano, G., Mallamace, F., Migliardo, P., & Wanderlingh, F. (1981). Raman scattering and structure of normal and supercooled water. *The journal of chemical physics*, 75(9), 4264-4270.
14. De Marco, L., Carpenter, W., Liu, H., Biswas, R., Bowman, J. M., & Tokmakoff, A. (2016). Differences in the vibrational dynamics of H₂O and D₂O: observation of symmetric and antisymmetric stretching vibrations in heavy water. *The Journal of Physical Chemistry Letters*, 7(10), 1769-1774.
15. Đuričković, I., Claverie, R., Bourson, P., Marchetti, M., Chassot, J. M., & Fontana, M. D. (2011). Water-ice phase transition probed by Raman spectroscopy. *Journal of Raman Spectroscopy*, 42(6), 1408-1412.
16. Faurskov Nielsen, Ole (2001). Low-frequency Raman Spectroscopy and Biomolecular Dynamics: A Comparison between different low-frequency experimental Techniques. *Collectivity of Vibrational modes*. In Lewis, I. R., & Edwards, H. (2001). *Handbook of Raman spectroscopy: from the research laboratory to the process line*. CRC press.
17. Furić, K., Ciglencić, I., & Čosović, B. (2000). Raman spectroscopic study of sodium chloride water solutions. *Journal of Molecular Structure*, 550, 225-234.
18. Georgiev, G. M., Kalkanjiev, T. K., Petrov, V. P., Nickolov, Z., & Miteva, M. (1983). Concentration-dependence studies of Raman spectra of water by the method of self-deconvolution. *Chemical physics letters*, 103(1), 83-88.
19. Gopalakrishnan, S., Jungwirth, P., Tobias, D. J., & Allen, H. C. (2005). Air-liquid interfaces of aqueous solutions containing ammonium and sulfate: Spectroscopic and molecular dynamics studies. *The Journal of Physical Chemistry B*, 109(18), 8861-8872.
20. Hanel, R., Thurner, S., & Tsallis, C. (2009). Limit distributions of scale-invariant probabilistic models of correlated random variables with the q-Gaussian as an explicit example. *The European Physical Journal B*, 72(2), 263.
21. Hare, D. E., & Sorensen, C. M. (1992). Interscillator coupling effects on the OH stretching band of liquid water. *The Journal of chemical physics*, 96(1), 13-22.
22. Hu, Q., Lü, X., Lu, W., Chen, Y., & Liu, H. (2013). An extensive study on Raman spectra of water from 253 to 753 K at 30 MPa: A new insight into structure of water. *Journal of Molecular Spectroscopy*, 292, 23-27.
23. 'Isosbestic point' in IUPAC Compendium of Chemical Terminology, 3rd ed. International Union of Pure and Applied Chemistry; 2006. Online version 3.0.1, 2019. <https://doi.org/10.1351/goldbook.I03310>
24. Jansen, T. L. C., Hayashi, T., Zhuang, W., & Mukamel, S. (2005). Stochastic Liouville equations for hydrogen-bonding fluctuations and their signatures in two-dimensional vibrational spectroscopy of water. *The Journal of chemical physics*, 123(11).
25. Kargovsky, A. V. (2006). On temperature dependence of the valence band in the Raman spectrum of liquid water. *Laser Physics Letters*, 3(12), 567.
26. Keutsch, F. N., & Saykally, R. J. (2001). Water clusters: Untangling the mysteries of the liquid, one molecule at a time. *Proceedings of the National Academy of Sciences of the United States of America*, 98(19), 10,533-10,540. <https://doi.org/10.1073/pnas.191266498>
27. Kubo, R. (1969). A stochastic theory of line shape. *Advances in chemical physics*, 15, 101-127.
28. Li, R., Jiang, Z., Shi, S., & Yang, H. (2003). Raman spectra and ¹⁷O NMR study effects of CaCl₂ and MgCl₂ on water structure. *Journal of Molecular Structure*, 645(1), 69-75.
29. Li, R., Jiang, Z., Chen, F., Yang, H., & Guan, Y. (2004). Hydrogen bonded structure of water and aqueous solutions of sodium halides: a Raman spectroscopic study. *Journal of molecular structure*, 707(1-3), 83-88.
30. Long, D. A. (2002). *The Raman effect*. John Wiley & Sons Ltd.
31. Ludwig, R. (2001). *Water: From clusters to the bulk*. *Angewandte Chemie International Edition*, 40(10), 1808-1827.
32. Maeda, Y., & Kitano, H. (1995). The structure of water in polymer systems as revealed by Raman spectroscopy. *Spectrochimica Acta Part A: Molecular and Biomolecular Spectroscopy*, 51(14), 2433-2446.
33. Malfait, B., Moréac, A., Jani, A., Lefort, R., Huber, P., Fröba, M., & Morineau, D. (2022). Structure of water at hydrophilic and hydrophobic interfaces: Raman spectroscopy of water confined in periodic mesoporous (organo) silicas. *The Journal of Physical Chemistry C*, 126(7), 3520-3531.
34. Monosmith, W. B., & Walrafen, G. E. (1984). Temperature dependence of the Raman OH-stretching overtone from liquid water. *The Journal of chemical physics*, 81(2), 669-674.
35. Paarmann, A., Hayashi, T., Mukamel, S., & Miller, R. J. D. (2008). Probing intermolecular couplings in liquid water with two-dimensional infrared photon echo spectroscopy. *The Journal of chemical physics*, 128(19).
36. Pershin, S. M., Lednev, V. N., Yulmetov, R. N., Klinkov, V. K., & Bunkin, A. F. (2015). Transparent material thickness measurements by Raman scattering. *Applied Optics*, 54(19), 5943-5948.
37. Porezag, D., & Pederson, M. R. (1996). Infrared intensities and Raman-scattering activities within density-functional theory. *Physical Review B*, 54(11), 7830.
38. Rull, F. (2002). Structural investigation of water and aqueous solutions by Raman spectroscopy. *Pure and applied chemistry*, 74(10), 1859-1870.
39. Sceats, M. G., Stavola, M., & Rice, S. A. (1979). On the role of Fermi resonance in the spectrum of water in its condensed phases. *The Journal of Chemical Physics*, 71(2), 983-990.
40. Scherer, J. R., Go, M. K., & Kint, S. (1973). Raman spectra and structure of water in dimethyl sulfoxide. *The Journal of Physical Chemistry*, 77(17), 2108-2117.

41. Scherer, J. R., Go, M. K., & Kint, S. (1974). Raman spectra and structure of water from -10 to 90. deg. *The Journal of Physical Chemistry*, 78(13), 1304-1313.
42. Schmidt, D. A., & Miki, K. (2007). Structural correlations in liquid water: a new interpretation of IR spectroscopy. *The journal of physical chemistry A*, 111(40), 10119-10122.
43. Skinner, J. L., Auer, B. M., & Lin, Y. S. (2009). Vibrational line shapes, spectral diffusion, and hydrogen bonding in liquid water. *Advances in Chemical Physics*, 142, 59.
44. Smith, J. D., Cappa, C. D., Wilson, K. R., Cohen, R. C., Geissler, P. L., & Saykally, R. J. (2005). Unified description of temperature-dependent hydrogen-bond rearrangements in liquid water. *Proceedings of the National Academy of Sciences of the United States of America*, 40, 14,171-14,174.
45. Smith, E., & Dent, G. (2019). *Modern Raman spectroscopy: a practical approach*. John Wiley & Sons.
46. Sparavigna, A. C. (2022). Entropies and Logarithms. Zenodo. DOI 10.5281/zenodo.7007520
47. Sparavigna, A. C. (2023). Role of Lyotropic Liquid Crystals in Templating Mesosilica Materials. *International Journal of Sciences*, 12(07), 7-40.
48. Sparavigna, A. C. (2023). q-Gaussian Tsallis Line Shapes and Raman Spectral Bands. *International Journal of Sciences*, 12(03), 27-40.
49. Sparavigna, A. C. (2023). q-Gaussian Tsallis Line Shapes for Raman Spectroscopy (June 7, 2023). SSRN Electronic Journal. <http://dx.doi.org/10.2139/ssrn.4445044>
50. Sparavigna, A. C. (2023). Tsallis q-Gaussian function as fitting lineshape for Graphite Raman bands. ChemRxiv. Cambridge: Cambridge Open Engage; 2023.
51. Sparavigna, A. C. (2023). SERS Spectral Bands of L-Cysteine, Cysteamine and Homocysteine Fitted by Tsallis q-Gaussian Functions. *International Journal of Sciences*, 12(09), 14-24. <https://doi.org/10.18483/ijsci.2721>
52. Sparavigna, A. C. (2024). Kubo Lineshape and its Fitted q-Gaussian Tsallis Function. *International Journal of Sciences*, 13(01), 1-9.
53. Sparavigna, A. C. (2024). Water, q-Gaussians and Raman Spectroscopy, *International Journal of Sciences* 03:17-25 DOI: 10.18483/ijSci.2751
54. Sun, Q. (2009). The Raman OH stretching bands of liquid water. *Vibrational Spectroscopy*, 51(2), 213-217.
55. Sun, Q. (2010). The single donator-single acceptor hydrogen bonding structure in water probed by Raman spectroscopy. *The Journal of chemical physics*, 132(5).
56. Tokmakoff, A. (2014) *Time-Dependent Quantum Mechanics and Spectroscopy*. Univ. Chicago. <http://tdqms.uchicago.edu/>
57. Torii, H. (2006). Time-domain calculations of the polarized Raman spectra, the transient infrared absorption anisotropy, and the extent of delocalization of the OH stretching mode of liquid water. *The Journal of Physical Chemistry A*, 110(30), 9469-9477.
58. Tsallis, C. (1988). Possible generalization of Boltzmann-Gibbs statistics. *Journal of statistical physics*, 52, 479-487.
59. Tsallis, C. (1995). Some comments on Boltzmann-Gibbs statistical mechanics. *Chaos, Solitons & Fractals*, 6, 539-559.
60. Tikhvatullin, F. H., Pogorelov, V. Y., Jumabaev, A., Hushvaktov, H. A., Absanov, A. A., & Usarov, A. (2011). Polarized components of Raman spectra of O-H vibrations in liquid water. *Journal of Molecular liquids*, 160(2), 88-93.
61. Umarov, S., Tsallis, C., Steinberg, S. (2008). On a q-Central Limit Theorem Consistent with Nonextensive Statistical Mechanics. *Milan J. Math. Birkhauser Verlag*. 76: 307-328.
62. Walrafen, G. E. (1964). Raman spectral studies of water structure. *The Journal of Chemical Physics*, 40(11), 3249-3256. <https://doi.org/10.1063/1.1724992>
63. Walrafen, G. E. (1967). Raman spectral studies of the effects of temperature on water structure. *The Journal of Chemical Physics*, 47(1), 114-126. <https://doi.org/10.1063/1.1711834>
64. Walrafen, G. E. (1968). Raman spectral studies of HDO in H₂O. *The Journal of Chemical Physics*, 48(1), 244-251.
65. Walrafen, G. E., Hokmadabi, M. S., & Yang, W.-H. (1986). Raman isosbestic points from liquid water. *The Journal of Chemical Physics*, 85(12), 6964-6969. <https://doi.org/10.1063/1.451383>
66. Wang, Z., Pakoulev, A., Pang, Y., & Dlott, D. D. (2003). Vibrational substructure in the OH stretching band of water. *Chemical physics letters*, 378(3-4), 281-288.
67. Zhelyaskov, V., Georgiev, G., Nickolov, Z., & Miteva, M. (1989). Concentration (D₂O in H₂O) and temperature Raman study of the molecular interactions in the OD stretching spectra of D₂O and D₂O/H₂O mixtures using the fourier deconvolution technique. *Journal of Raman spectroscopy*, 20(2), 67-75.